TEAM GREEN
Astrophysical Research Initiative for Space Telescopic Observations of Transiting Large Exoplanets (ARISTOTLE)

Majdi Assaid, Frederik Dall'Omo, Cara Doumbe Kingue, Yoshi N. E. Eschen, Frankie Falksohn, Angelos Georgakis, Fabian Hauser, Adam Hlacik, Jonas G. S. Lunde, Josephine Maglio, Willeke Mulder, Jota Navarro Fernández, Marie Puissant, Rick Röthlisberger and Einari Toivonen.

Tutors: Gabby Aitink-Kroes and Christian Gritzner

Abstract

There are over 4000 exoplanets detected by transits, with many more likely to be added soon. Only around 100 of them have characterised atmospheres, a key component in understanding important planetary aspects, like habitability. ARISTOTLE aims to address this discrepancy by performing the largest transit spectrophotometric survey to date to characterise the atmospheres of exoplanets, down to Super-Earths, in the mid-infrared (MIR). With a 4m dish and a spectrographic resolution of R=100-200 up to 23µm, one of the missions primarily focuses will be the exoplanets to be detected by the planned PLATO mission, which are believed to include many terrestrial planets. ARISTOTLE will also perform secondary eclipse spectroscopy and phase-curve analysis, as well as study the formation of planetary systems through MIR direct imaging of planetary disks. Lastly, the mission aims to enhance our understanding of the solar system by conducting further studies on Uranus, Neptune, and the moons and comets within our own solar system, as an indirect way of widening our understanding of exoplanets.

1 Introduction

Previous, ongoing, and future exoplanet missions such as Kepler [8], TESS [24], and PLATO [27] have and will detect exoplanets using the transit method. These exoplanets vary in their period, radius, temperature, semi-major axis, environment and composition. So far follow-ups to characterise their atmospheres have been performed on roughly 100 planets (see Figure 1)

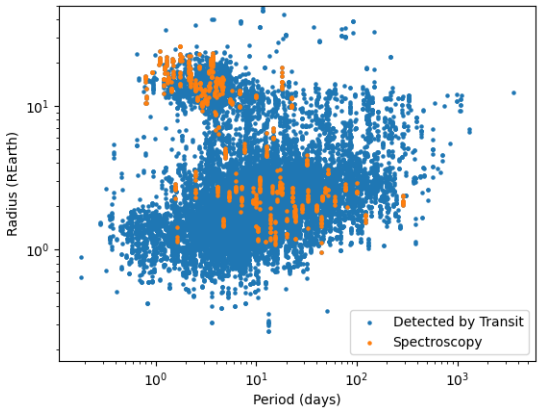

Figure 1: There are around 4000 exoplanets detected by transit (blue) and around 100 exoplanets characterised by transmission/emission spectroscopy (orange) to date[1].

While the Kepler and the K2 missions have ended, TESS will still be finding new transiting exoplanets over the next years (currently EM2) [30]. The PLATO mission is planned to be launched by the end of 2026 and will among with other things find more Earth-like planets [5]. By the year 2029 ARIEL will be launched with the aim to characterise atmospheres of warm and hot planets down to close, hot Super-Earths [26]. The ARISTOTLE mission will launch in 2035, and target previously identified exoplanets, characterising them based on (bio)signatures and other molecules in the MIR. These exoplanets will range from cold to hot, and in sizes from Jupiter-sized planets down to smaller, rocky ones.

[1]Determined by the data available on https://exoplanetarchive.ipac.caltech.edu/ accessed on 18. July 2023

2 Science

The scientific questions asked by the Aristotle mission, together with the objectives required to answer these questions, are summarised in table 1. Section 2.1 will present the missions primary science case, while Section 2.2 presents the secondary science cases.

2.1 Primary Science Case

ARISTOTLE's primary science case is the characterisation of exoplanet atmospheres, primarily through transits, combined with eclipses and phase-curve observations for selected planets. As demonstrated in Figure 1, the vast majority of known transiting planets have not had their atmospheres characterised. Even though other mission, such as ARIEL and JWST's instrument MIRI are helping to put a dent in these figures, they are, respectively, limited in their frequency range and photon collection capabilities (ARIEL), and available observation schedule (JWST). Additionally, the PLATO mission will soon help populate the number of observed but not atmospherically characterised planets even further, especially in the Earth-like regime. ARISTOTLES's large dish, wide frequency band, and high thermal performance will allow it to characterise fainter and colder plan-

Primary science question	Primary science objectives
Q1: Under what conditions are exoplanet atmospheres possible, and how do these shape their characteristics?	**O1.1**: Tracing and identifying photochemistry in exoplanetary atmospheres down to Super-Earths around Sun-like stars. **O1.2**: Cross-correlate and break ARIEL degeneracies, by going to higher wavelengths. **O1.3**: Probe M-star and Sun-like star systems over multiple transits to properly understand both the host star and the full phase curve in large detail.
Secondary science questions	**Secondary science objectives**
Q2: How do planetary systems form and evolve?	**O2.1:** The mission shall observe young protoplanetary / young circumstellar disks to help understand the evolution of stellar systems. **O2.2:** The mission shall observe the thermal emissions of further out exoplanets.
Q3: How does our solar system work, and does it compare to other stellar systems?	**O3.1:** Understanding the atmospheric dynamics of solar system gas planets by constraining their energy budget through observations of thermal emissions of the lower atmosphere. **O3.2:** Constraining the elemental abundances during the early age of our solar system by looking at pristine comets.
Q4: Is there life elsewhere in our solar system?	**O4.1:** Synergise with other missions by looking for biosignatures in solar system moons which are undiscovered so far. (O3.2 applies here as well).

Table 1: ARISTOTLE science cases. Left: Science questions our mission aims to answer. Right: Objectives we aim to achieve in order to answer these questions.

ets than ARIEL, which is estimated to be photon noise limited when observing faint targets [15]. However, the overlapping frequency with ARIEL ($2.5-7.8\mu m$) presents a great opportunity for cross-experiment calibration, and better understanding of biases and systematics of both experiments. At the same time, ARISTOTLE's higher wavelengths ($7.8-23\mu m$) can break known degeneracies between spectral lines in ARIEL's frequency range.

2.1.1 Observational Paradigms

ARISTOTLE's primary science revolves around three common observational methods for exoplanet characterisation:

Transit Spectroscopy: During transit events, stellar radiation penetrates through the potentially existing atmospheres of exoplanets [43], with molecules absorbing specific frequencies of the radiation in the MIR to excite their vibrational fingerprints [17]. This allows us to determine the absorption spectra of the exoplanet's atmospheres, constraining molecular abundances in the atmosphere [4].

Secondary Eclipse Spectroscopy: When exoplanets pass behind their host stars during their orbits, the emission from the exoplanet disappears from the spatially unresolved joint spectrum. Comparing the eclipse to the joint spectrum right before the eclipse allows for the determination of the emission spectrum from the exoplanet itself, which in turn reveals the absorption spectrum and molecular abundances in the atmosphere [31].

Phase Curves: The transit and eclipse observations can be extended to observing the phase-curve of the planet through its entire orbit. While this is time-consuming, it allows for fitting and constraining anisotropies and rotational features of the planet. Through variations in these phase curves, clouds in the atmospheres of the exoplanets can be determined [18].

2.1.2 Spectral Lines and Biosignatures

A number of interesting spectral lines, many of which are biosignatures, fall within the ARISTOTLE frequency range ($2.5-23\mu m$), as seen in Figure 2. The mission plans to extensively study:

- Chemical disequilibria between O_3 (14.5µm), an indirect O_2 marker, and CH_4 (7.6-7.7µm) [40].

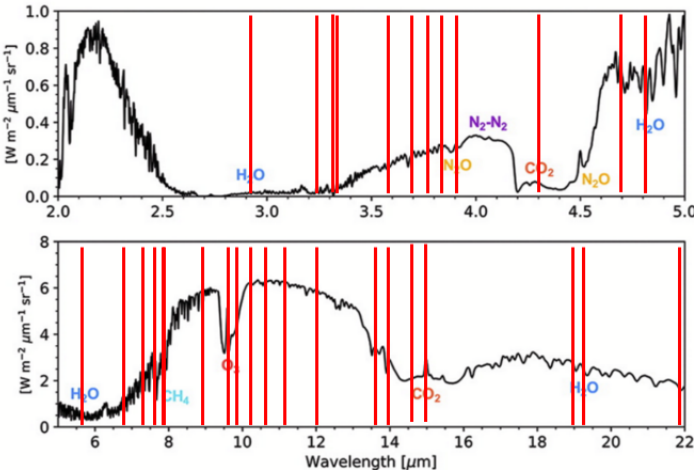

Figure 2: Illustration of the absorption spectrum of Earth's atmosphere across the ARISTOTLE frequency range. The red lines indicate interesting (bio)signatures. Figure adapted from Schwieterman [22]

- Climate and volcanic dynamics through the interactions between CO_2 (15µm), N_2O (17µm), SO_2 (19µm), CO (4.7µm) and H_2S (3.7-3.9µm) [40].
- Suspected molecular precursors of life like HCN [11] (14µm) and hydrocarbons [7] such as C_2H_4 (10.6µm), C_3H_8 (13.6µm), C_2H_2 (13.7µm) and C_2H_6 (3.5, 6.8, and 12µm).
- Potential biosignatures from H2-dominated atmospheres, namely PH_3 (10µm) and NH_3 (10.5µm) [42] [45].
- Key molecules to sustain life as we know it on Earth: H_2O (22µm) and N_2 (4.3µm) [40] [11].
- Promising phyllosilicates, such as Serpentine (10µm), Kaolinite (9 and 14µm), Montmorillonite (10 and 14µm) and Illite (10 and 14µm). These minerals are thought to impact geologic and overall atmospheric formations [41].

The aim of these studies is to gather comprehensive data on (bio)signatures and assess the potential habitability of exoplanets by analyzing their atmospheres. By examining a wider range of wavelengths, the ARISTOTLE project will not only enable

the detection and verification of crucial atmospheric compounds but also provide in-depth insights into molecular overlaps and their relevance in both biological and non-biological processes.

2.1.3 Planet Selection

ARISTOTLE will study a wide range of planet types, focusing on G and K star systems. However, a relatively large proportion of the observational time will be dedicated to repeated transits, eclipses, and phase curve observations of select interesting systems, like habitable zone planets and Super-Earths. The planet selection will depend on the findings of the PLATO mission, and substantial observation time would be allocated if a transiting terrestrial planet were found in the habitable zone of a system close enough for it to be characterised (or at the very least, it's black-body temperature constrained) by ARISTOTLE. Other high-priority targets for substantial characterisation are Sub-Neptune's in the habitable zone, which, with their much deeper atmospheres compared to rocky planets, are easier to observe in transit. Although targeting PLATO findings, if PLATO were to fail, ARISTOTLE can still follow up on a plethora of TESS targets that could not be characterised by ARIEL.

2.2 Secondary Science Cases

2.2.1 Protoplanetary Disks

Protoplanetary disks are expected to re-emit a large fraction of the stellar flux in the infrared [14]. Combining MIR imaging with observations at other wavelengths allows us to further constrain disk properties and even search for thermal emission from (planetary) companions. Especially if the companions in the system still have circumplanetary disks (CPDs), which are expected to be bright in the MIR. MIR observations of protoplanetary disks from space are favourable over those from the ground for the following reasons:

- We are looking for faint sources in the 2.2 - 23 µm range. Observations with ground-based telescopes are limited due to the atmosphere's thermal background [12] [13] [32]. The low thermal background of ARISTOTLE will provide unprecedented sensitivity for these sources. With ARISTOTLE, we aim for a 250 times better sensitivities than the Near Earths in the AlphaCen Region (NEAR [29]) instrument on the VLT Imager.
- The stellar spectrum decreases rapidly with wavelength ($\propto \lambda^{-4}$), resulting in a higher contrast of exoplanets with respect to their host star in the MIR. However, typical stellar spectra at these wavelengths convey atomic absorption lines, which will not correlate with the exoplanet atmosphere signatures that are mostly dominated by molecules [9].

We are interested in targets that have been observed as part of the NEAR experiment: HD 100546, HD 163296, HD 169142, TW Hydra, HD 100453, HD 36112 [13], and even potentially habitable planets around both components of the binary Alpha Centauri [29] [28].

2.2.2 Lower Atmospheres of Uranus and Neptune

Uranus and Neptune are two planets in our Solar System with lower atmospheres that are largely unexplored by other missions. Measurements of the surface temperature, planetary flux, atmosphere composition, and more can be obtained by analysing the lower atmospheres of the planets [36]. Imaging the planets at longer wavelengths than other missions would allow one to peer into lower atmospheres that are largely unexplored. This allows us to calculate the energy budget, which describes the difference between the incoming radiant energy and the outgoing thermal energy for the planet [44]. With this information, the climate and heat transportation of the planets can be explored as they are highly dependent on the balance of the energy budget. Uranus and Neptune share similarities with many exoplanets that have been detected [37], and understanding the planets in our own Solar System can thus help us understand exoplanets of similar size and composition.

2.2.3 Solar System Moons

Moons with an icy surface are of particular interest in the search for extraterrestrial life. Some are thought to have a subsurface ocean and a rocky core; combined with atmospheres comparable to the prebiotic Earth, could indicate the presence of extremophilic microorganisms beneath their surface. Until now, missions have mainly focused on UV and near-IR observations, consequently mid-IR over 10 µm would allow a more extensive study of:

- 'Classic' life-associated molecules such as CO_2
- SO_2, a marker of geothermal activity
- Hydrocarbons, markers of potential primordial life

Our work on atmospheric compositions and dynamics in moons of the Solar System will not only bring a complementary layer of information to the JUICE (Jupiter Icy Moons Explorer) mission, but will also set bases for the ongoing study of exomoons [35] [6] [38].

2.2.4 Solar System Comets

In our Solar System we also find other celestial bodies such as comets. They orbit the Sun at a great range of distances and consist of leftover building blocks of the outer Solar System formation processes [3]. Pristine comets are of special interest as their constitutions are relatively preserved. Oort Cloud comets seem to specifically be more pristine and less processed than comets originating from the Jupiter-family, with differences in the silicate compositions being reported [21]. These differences would be of interest to the mission as most silicates seem to have spectral lines above 10 µm. More complex organic molecules such as hydrocarbons (e.g. C_2H_2) that can be observed at longer wavelengths would also be of particular interest to observe [39]. By studying comets we can gain valuable insights into how our Solar System formed and the molecules that might have been the basis for life on Earth itself. This can in turn help us when we look for signs of life on exoplanets in other planetary systems.

3 Science Requirements

We have defined the following scientific requirements for our instrument, to be able to fulfill our scientific objectives, divided into primary (PSR) and secondary scientific requirements (SSR):

1. PSR1: The mission shall do spectrography in the range of $2.5 - 23 \mu m$.
2. PSR2: The spectrograph shall have a resolution R=200 ($2.5 - 10 \mu m$) and R=100 ($10 - 23 \mu m$).
3. PSR3: The mission shall be able to observe continuously for up to 24 hours.

Noise type	Source/Description	Error estimate (ppm)	Mitigation
Photon noise	Statistical noise from the finite number of photons observed.	0.8 - 6 ppm (increasing with λ)	Large mirror size, long observations of faint targets.
Dish thermal emission	Photons emitted by the grey-body telescope dish.	0 - 3 ppm (increasing with λ)	Cold-stop in optics, <100K dish temperature.
Zodiacal background	Sunlight scattered by interplanetary dust.	0 - 5 ppm (increasing with λ)	Improved modelling.
Stellar variability	Stochastic star variability, mostly due to granulation.	~2 ppm (possibly decreasing with λ)	Long observations to properly understand star.
Pointing jitter	Instability of pointing when tracking a source on the spectrograph.	~1 ppm	Low-thrust micro-propulsion system.
Dark current	Current leakage from the CCD, caused by its temperature.	~0ppm for spectrograph (high readout) < 2 ppm for imager	Low detector temperatures.
Read noise	Error in number of electrons on CCD readout.	~0 ppm for bright targets	Quickly integrates down with multiple readouts.
Calibration stability & fringes	Imperfection in pixel response, interference in detectors.	< 5 ppm (target. down from MIRI 25ppm)	Detector development, learning from MIRI, long timescale systematics analysis.

Table 2: Summary of primary noise sources, their roughly estimated error in parts per million (ppm), and employed mitigation techniques. Error estimates are (where applicable) scaled to observations of transits of a Sun-like star at 50 pc over 100 hours. Photon noise is calculated from first principles with Poisson statistics, while most of the other sources are scaled and approximated from similar instruments, like JWST MIRI[23], ARIEL[15], PLATO[19], and Origins[31].

4. PSR4: The mission shall be able to observe up to 5 transits of exoplanets in the habitable zone of sun-like stars.

5. SSR1: The imager shall have a spatial resolution of 50AU at 100pc (R = 500mas).

6. SSR2: The imager shall have a coronagraph.

7. SSR3: The mission shall be able to image in 10.65, 11.4, 15.5, 19, 22 μm bands.

8. SSR4: The mission shall image with less than 50mas relative pointing error.

3.1 Noise Estimation and Mitigation

ARISTOTLE relies on high precision spectrophotometry, requiring proper understanding and mitigation of all relevant error sources within and outside our instrument. A preliminary summary and estimate of these can be found in Table 2. As we can see, no single noise source is believed to be dominant, indicating a well-balanced instrument for our primary science case. Our target error level for our most sensitive measurements (series of transitions or eclipses of faint planets) is ~5 ppm. At this level, a few error sources don't necessarily integrate down in a statistical sense with increased integration time, notably stellar activity and detector fringes. An important part of the ARISTOTLE sensitivity target is therefore repeated transits of high-priority planets, from which we can quantitatively study both stellar activity and our own instrument.

Granulation, flares, and other stellar activity can be erratic, and require careful monitoring and mitigation. For reference PLATO has predicted a 2 ppm per transit from stellar granulation[19]. This effect is predicted to diminish at higher wavelengths.

Detector fringes and calibration errors also do not necessarily integrate down with time. This is one of the main precision limitations of JWST's MIRI, with reported flux errors of up to 30%[20], mitigated to < 25ppm levels with post-processing[25]. This problem presents extensive room for improvement, both in detector development, and in the understanding and mitigation of these effects. While JWST distributes its time between many instruments and targets, ARISTOTLE will dedicate large parts of its observational schedule to repeated transits, allowing for a much better understanding of our instrument systematics.

4 Mission Profile & Payload

In order to fulfill the requirements of the mission, we are going to follow the schedule shown in Figure 3 with the planned launch date of2035.

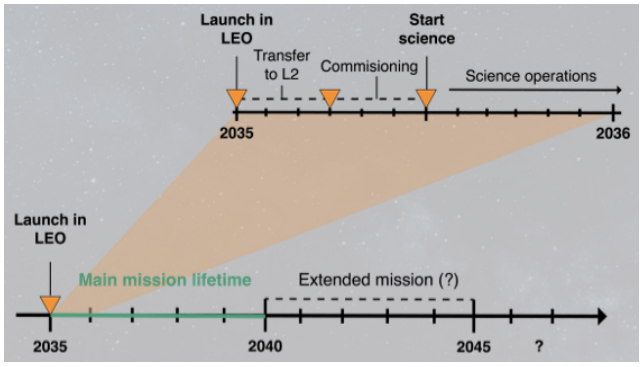

Figure 3: Concept of operations of ARISTOTLE mission

To meet the science objectives and the mission profile, the payload consists of the following instruments and supporting optic systems. This includes the pre-optics, imager and spectrograph as shown below:

4.1 Instruments

Pre-optics

- Tip Til Mirror (TTM): Stabilises the beam variations in the incoming beam and detected by the FGS performing tip tilt micro adjustments in the mirror.

- Cold Stop (CS): Is designed to match the exit pupil of the telescope and thus avoiding parasitic radiation of telescope structures and background.

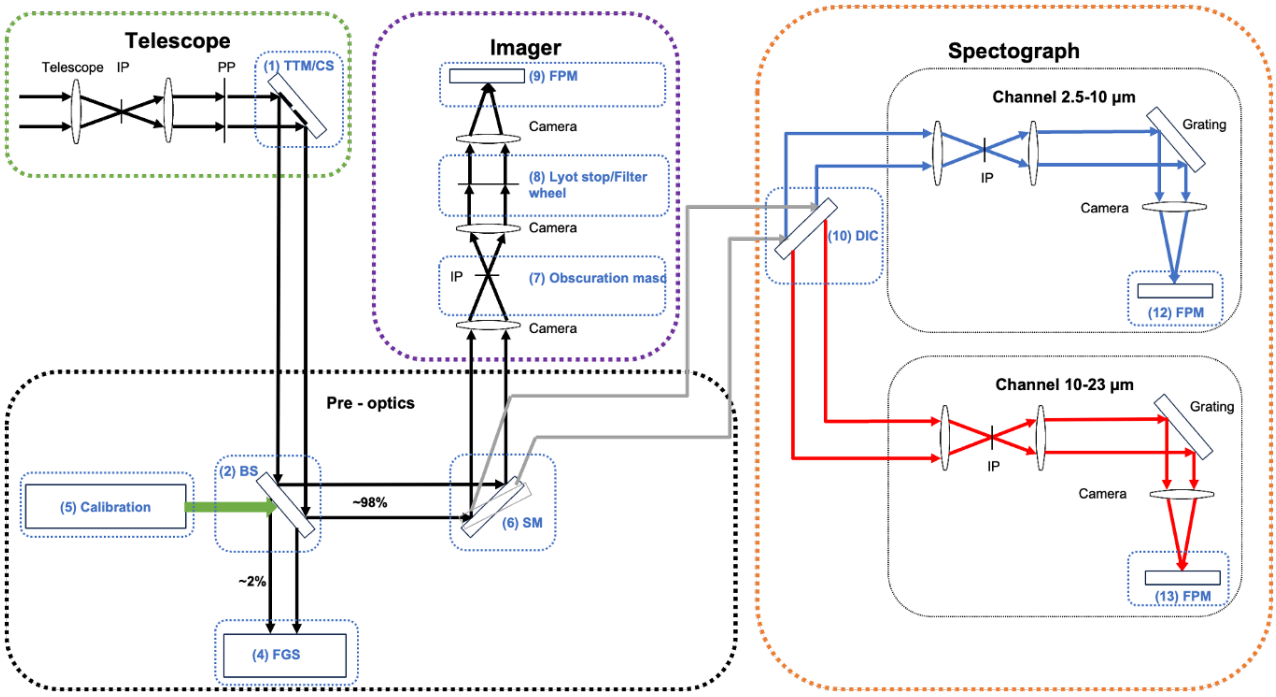

Figure 4: Lightpath from the telescope through the pre-optics ending in either the imager or spectrograph

- Beam Splitter (BS): To split the beam in 2% for the FGS and directs the remaining 98% of the beam into the instruments.
- Selection Mirror (SM): This two position tilt mirror will direct the light into either the imager or spectrograph so that we have the flexibility to use two different instruments (spectrometer and imager) but onl one at a time.
- Fine Guiding Sensor (FGS): The FGS is a simple imager to measure the telescope motion to be corrected with the TTM. It provides data for science attitude determination, fine pointing, and attitude stabilisation in the focal plane.
- Calibration System: Will provide a well known signal using a hot Tungsten wire as a reference point as the emission lines are well known. Will complete calibrations separately to the measurements so as not to impact the data set.

Imager

- Obscuration Mask (OM): This is the main component of the coronagraph and is used to block out the central light of the star to enable the imager to detect surrounding bodies. It will be mounted on a system in before the filter wheel so a range of filter options can be used either with or without the obscuration mask. The mask will be perfectly centered in the field of view but can be switched 'on' and 'off' by utilising a bystable electromagnetic system.
- Filter Wheel (FW): The imager will have a filter wheel with a variety of filter options to support our range of science applications. The FW has 12 positions one open, a Lyot Stop (LS) to eliminate the diffraction effects of the centrel obscuration, five narrow band filters for multi wavelength imaging and lyot stopand narrow band filter combinations for narrowband spectoscrophy.

Spectrograph

- Houses two separate channels, each with a dispersive element and a FPM. The first channel will cover wavelengths from 2.5 µm - 10 µm at a higher resolution ($R = 200$) and the second channel will cover wavelengths from 10 µm - 23 µm at a lower resolution ($R = 100$)
- Focal Plane Module (FPM): The FPM is the detector in the imager which captures the image from the telescope.
- Dichroic (DIC): A specialised wavelength splitter that separates the light with shorter wavelengths from the light with longer wavelengths so that the respective beams could be fed into the correct spectrometer module.

5 Orbit Selection

The orbit for the ARISTOTLE spacecraft is selected to optimise scientific outcomes while taking technical constraints into account. One of the primary considerations is to ensure that measurements conducted by the payload are not influenced by other MIR sources. This is crucial to obtain accurate and reliable scientific data. In addition to this, thermal stability is an essential consideration to ensure the proper functionality of the spacecraft's thermal control system. Eclipses (Earth and Moon) avoidance ensures uninterrupted power generation. To accommodate these specific requirements, a Lissajous orbit around Lagrange point 2 (L2) is selected. This is approximately 1.5 million kilometers away from Earth on the side opposite to the Sun.

The amplitudes of the orbit are chosen to minimise eclipse durations, thereby reducing the necessary ΔV manoeuvres to mitigate eclipses caused by the Moon or Earth. In the plane perpendicular to the ecliptic, the amplitudes of the orbit are 800,000 kilometers in the y-direction, 400,000 kilometers in the z-direction, and 230,000 kilometers in the x-direction within the ecliptic. (see Figure 5). The transfer to the L2 point takes 94 days and one orbit around the L2 takes 182 days.

In order to reach L2, two orbital manoeuvres are necessary after launcher separation. The first manoeuvre, known as the

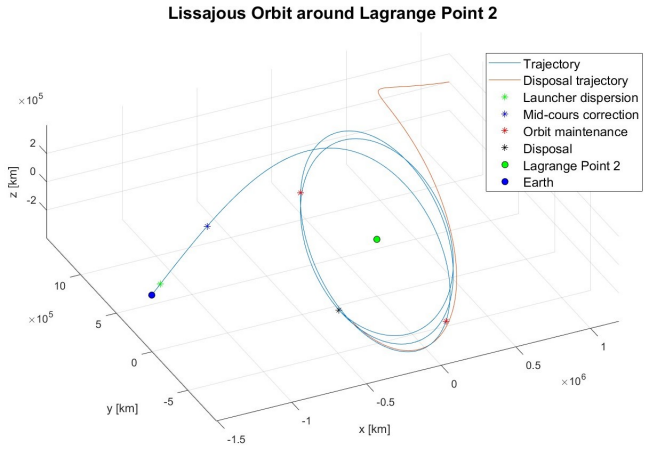

Figure 5: Spacecraft trajectory and required manoeuvres for orbiting at Lagrange point 2

launcher dispersal manoeuvre, is conducted to account for any launch inaccuracies. This manoeuvre is executed shortly after the spacecraft separation from the launch vehicle. Due to the high sensitivity of the final trajectory at L2 to initial conditions, an additional mid-course manoeuvre is performed. Due to the instability of orbits around the L2 point, frequent orbit maintenance manoeuvres are required. To prevent entering an eclipse additional eclipse manoeuvres are conducted.

The mission follows the ESA space debris mitigation guidelines [1] for the disposal of the spacecraft. To accomplish this, a final manoeuvre is conducted, placing the spacecraft on a heliocentric disposal orbit. This disposal orbit is designed to ensure that the spacecraft will not revisit Earth at a closer distance than 1.5 million kilometers within the next 100 years. The ΔV values are shown in Figure 5).

ΔV Manoeuvres	ΔV
Removal launcher dispersion	50 m/s
Mid-course correction	1 m/s
Orbit maintenance (for 5 years)	10 m/s
Eclipse correction	10 m/s
Disposal	20 m/s
Total	**91 m/s**

Table 3: ΔV budget for mission life time of 5 years

6 Radiation Considerations and Shielding

The L2 orbit chosen for the ARISTOTLE mission lies outside of the Van Allen belt, which is a concentrated zone of charged particles that are captured from the solar wind and held around Earth by the planets magnetosphere. At the L2 position, the main source of radiation comes from protons from solar flares or the cosmic background radiation. For this reason, the radiation shielding does not have to be as rigorous as it would have to be for other orbit locations. This has been demonstrated by Gaia, a mission also occupying the L2 orbit, which has had its radiation damage recently evaluated and is thought to have suffered damage an order of magnitude lower than was originally predicted. [33] For this reason, the shielding for ARISTOTLE will be based on the shielding used in the Gaia mission, which includes:

- Ensuring the spacecraft is built from materials that have been tested to shield from radiation.
- The electrical components are hardened against radiation

Additional radiation shields have been included into the design of the spacecraft. In addition to all of these measures, if, during ground testing, it has been determined that some of the more fragile electronic components are likely to sustain considerable radiation damage, there is an option to include additional triple layer shields. These shields consist of a layer of Molybdenum (a dense material which is effective for shielding against high energy x-rays and gamma rays) sandwiched between two layers of bronze aluminium alloys (effective lightweight shielding which will act to reduce the effect of secondary particles from the irradiated Molybdenum from damaging the electrical components). [10]

7 Telescope Structure

The structure of the telescope is designed to provide an optimal environment, structural integrity and ensure the proper functioning of the payload. Together, the subsystems provide power, shielding to the environment and communication with the Earth. In addition to linking the different subsystems to the payload, the spacecraft structure ensures mechanical support and load carrying.

7.1 Mechanical Support

The structure is studied to support the mechanical loads expected from the different phases of the telescope's life, the most critical one being the launch. The second consideration is the fairing size of Ariane 6, which limits the diameter of the whole telescope. The eigenfrequencies of each subsystem must also be contained in predetermined ranges that will be provided in the next phases of the design. This study ensures decoupling between the different parts and thus avoids damage to the structure and thus the payload.

7.2 Mechanisms

The pointing accuracy demanded by the science mission is notably obtained by the use of a mechanism tilting the telescope on demand. This flexibility is in addition to the pointing manoeuvres provided by the attitude control and propulsion systems.

One of the two solar panels is retractable to validate the diameter restriction given by the launcher. The same deployment is necessary for the thermal shield surrounding the primary and secondary mirrors. The technology required to perform such movements is heritage from Gaia.

7.3 Weight Evaluation

Table 4 shows the weight distribution in the system. A margin of 20% is taken for the less known technologies and configurations. A final 20% of margin is imposed to the total mass.

8 Thermal System

The thermal system must ensure that all the devices of the satellite are in their operational temperature range. The main requirements dictated by the primary science proposal are: the instrument bay temperature shall be $<8\,\mathrm{K}$ and the first and second mirror temperature shall be $<120\,\mathrm{K}$.

To achieve this, two cooling systems will be used:

SYSTEM	SUBSYSTEM	PART	MASS (Kg)		SYSTEM	SUBSYSTEM	PART	MASS (Kg)	
Telescope	Mirros	(M1 to M5)	460	460	**AOCS**	Rough pointing	Sensing	2	265
Instruments	Spectrograph		132	132			Actuators	12	
	Imager	Filter Wheel						150	
		Coronograph						12	
Structure	P/L structure	Support structure	400	400		Fine Pointing	Sensing	9	
	Bus structure		566	566				5	
Thermal	Active	P/L cryocooler unit	40	293			Actuators	75	
		BUS cooler unit	30		**Propulsion System**	Engine Unit	Thrusters	5	200
		Radiators	25				Tank	21	
		Plumbing	20			Tank	Green prop	171	
	Passive	MLI	132			Propellant	Solar arrays	13	
		Blanket Cover	15		**EPS**	Power	Batteries	11	145
		Buffer	31			Storage	Management	10	
Comms	Bi-TT&C	Radio(S-band)	5	40			PDU	15	
		Monopole antennas	5			Distribution	E Harness	100	
	One-P/L link	Radio	8				OBC	4	
		Dish	3		**DHS**		Storage	2	40
		Pointing mechanism	4				DPU	2	
							Data harness	30	
				MASS w/MARGIN	2525 Kg 3030 Kg				

Table 4: Mass budget evaluation

Passive Cooling System

A Multi-Layer Insulation (MLI) sun-shield will shade the telescope as well as the instruments module. It will have a semi-cylinder shape attached to the spacecraft during the launch that will be deployed during operation to cover the maximum possible surface from the radiation (see Figure 6).

Furthermore, two radiator panels will be placed away from the Sun rejecting the waste heat to space. The first one will be connected to the service module irradiating a heat power of $Q = 685\,W$ for which a surface of $a = 3.4\,m^2$ is required (this temperature will be controlled by heaters). The second one will be linked to the cooler of the instruments bay that is irradiating less power, $Q = 259\,W$. With this in mind, the instrument's segment will be cooler than the SVM. The area necessary for this power is $a = 1.3\,m^2$.

Active Cooling System

To compliment the passive cooling system, using JWST heritage, we will use a two-stage mechanical cryocooler. A pre-cooler system transfers the power using a Pulse-Tube to a Joule-Thomson [2] heat exchanger with which we will cover the temperature requirements for the instrument bay.

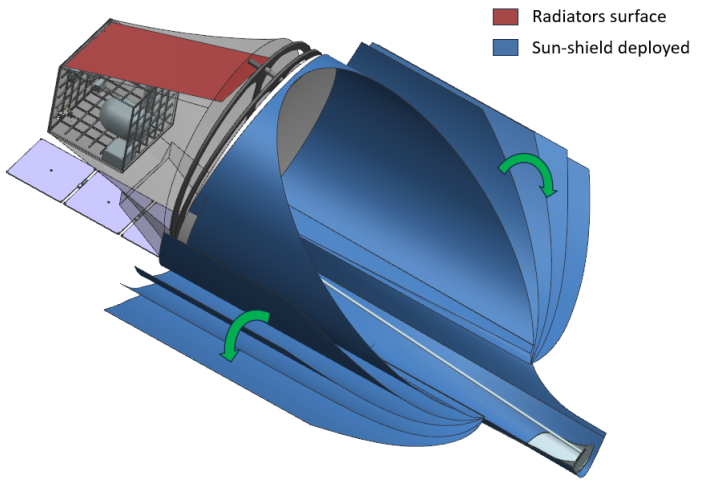

Figure 6: Spacecraft envelope highlighting the the passive cooling systems with the sun-shield deployed

9 Attitude and Orbit Control System

The Attitude and Orbit Control System (AOCS) will be in charge of the stability, pointing accuracy, attitude and orbital control of our spacecraft. To manage the requirements for the mission (Table 5), we will need the right devices:

For rough pointing, there will be 6 Sun sensors (+6 spare). Besides that, a Micro-Propulsion System (MPS) is deployed to ensure spin rate management of the reaction wheels and exceptional attitude stability during the scientific observations. Twelve cold-gas microthrusters with controllable thrust magnitude between 1 and 1000 µN micro-N, are deployed in two groups of 6. These thrusters have a specific impulse equal to Isp=290 and are strategically positioned throughout the spacecraft to provide precise actuation and the high level of precision required for optimal control of observation activities. Furthermore the Nitrogen tank supplying gas to the propulsion system will contain a total of 100 kg of fuel. This fuel quantity accounts for a 50% margin to ensure sufficient supply for the mission's needs.

On the other hand, for a fine pointing we will use four reaction wheels ($3 + 1$ spare) to control the primary axes of the spacecraft. Furthermore, to follow the science mission proposal, the spacecraft will have added 3 star-trackers that will full-fill the FOV necessary by analysing the positions of the stars to study.

Lastly, the Fine Guidance Sensor (FGS) is responsible for pointing precisely using a closed control loop. Our relative pointing error shall be $< 50\text{marcs}$ but, following the heritage of Hubble (10 marcs), and JWST (100 marcs), we will be able to obtain an accuracy of 30 milli-arcseconds. This will keep our spacecraft stable to obtain high-quality images.

AOCS parameters		
Rough pointing	Sensors accuracy	1.8 arcsec
	Actuators accuracy	>3000 arcsec
Fine Pointing	Sensors accuracy	30 marcsec
	Actuators accuracy	40 marcsec

Table 5: Parameters of AOCS to full-fill the mission requierements

10 Propulsion System

A chemical mono-propellant propulsion system has been selected to perform station keeping, orbit correction, and spacecraft disposal at the end of the mission. Hydrazine, which is considered the current state-of-the-art for similar space missions, has been identified as a substance of great concern by the REACH regulation in 2011. There is a significant possibility that these systems might be prohibited in the near future [34], as the chemical is highly toxic, mutagenic and carcinogenic for humans and harmful to the environment.

Our proposed propulsion system will use the LMP-103S, a non-toxic Green propellant that offers several advantages over Hydrazine, as it does not require such extensive safety precautions, which are both expensive and cumbersome. Furthermore, it has a 6% higher specific impulse and a density of $\rho = 1.24\,\mathrm{g\,cm^{-3}}$ [16] which is 24% higher than that of Hydrazine. The selected LMP-103S thrusters provide a nominal thrust at Beginning of Life (BoL) of 22 N, and a specific impulse of Isp = 250 s. According to ECAPS, the manufacturing company, these thrusters are currently undergoing a test fire campaign, in order to characterise their performance, advancing their TRL to 5/6. Four such thrusters are configured in two pairs, where in each pair one thruster is used to perform the ΔV manoeuvres and one is for redundancy.

For the nominal duration of the mission, which is five years, the total ΔV is estimated to $\Delta V = 91\,\mathrm{m\,s^{-1}}$, and the total firing time of the thrusters is estimated at 6347 s. For this, a total propellant mass of 114 kg is needed, and by considering a 50% of margin, the total propellant mass results to 171 kg of fuel that will be stored in a 140 litre tank located close to the main thrusters.

11 Telecommunication

The telecommunication system of the ARISTOTLE spacecraft comprises two independent systems: a low gain system and a medium gain system. The low gain system utilises S-band frequencies and is used for telecommanding, monitoring, and ranging. This system is equipped with two transceivers and two omnidirectional antennas positioned on opposite sides of the spacecraft to ensure communication in different attitudes. These redundancies enable reliable communication under varying orientations. Additionally, the transceivers are cross-coupled with the antennas and operate in hot redundancy, ensuring continuous communication even during emergency situations (see Figure 7 below). This system operates at a data rate of 2 kbits/s for downlink and 4 kbits/s for uplink.

The medium gain system uses X-band frequencies in conjunction with a medium gain parabolic dish antenna. The system incorporates redundancy by employing two transmitters operating in cold redundancy and using two amplifiers. (see Figure 7 top). The system yields an Effective Isotropic Radiated Power (EIRP) of 36 dB. This performance is well-suited to overcome the significant path transmission losses of approximately 236 dB from the L2 point to Earth. Additionally, it enables a downlink data rate of 10 Mbits/s while maintaining a link budget higher than 3 dB.

12 Data Handling

The ARISTOTLE spacecraft generates an average of 3 Gbit of data per day. However, during periods of condensed science measurements, the data production can peak at 33 Gbit per day. The instruments are only used one at a time, resulting in a significant reduction in the overall data generated during a measurement campaign. Due to a maximum data rate of 10 Mbits/s, only approximately 7 hours per week are needed to downlink the data.

Due to low data generation and frequent ground station contacts, no onboard data processing is necessary, thus, reducing the risk of data losses. An overview of the data generation can be seen in Table 6.

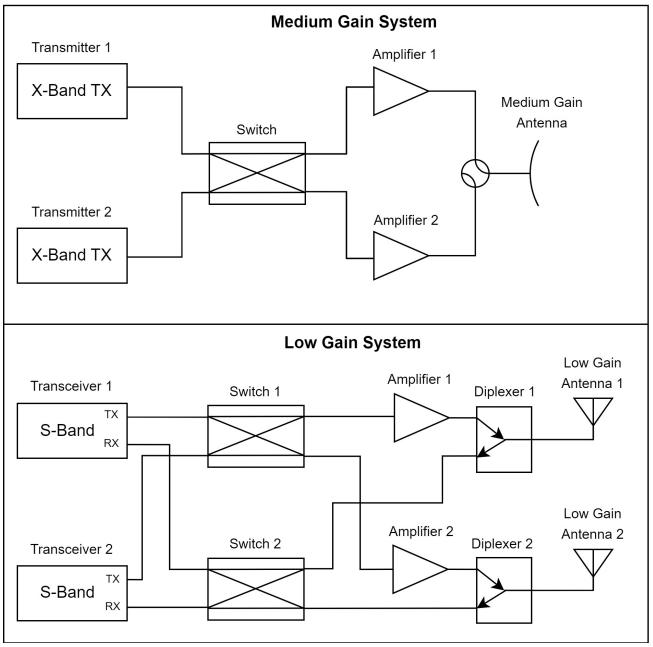

Figure 7: Telecommunication system for the ARISTOTLE spacecraft. Medium gain system (top) for telemetry and low gain system (bottom) for telecommanding, monitoring and ranging

Data produced	Average	Maximum
Spectrograph	2.7 Gbits/day	9 Gbits/day
Imager	4 Gbits/day	33 Gbits/day
Housekeeping	0.5 Gbits/day	-
Total	**3 Gbits/day**	**33 Gbits/day**

Table 6: Overview of data generation of different components

13 Power System

The power system is designed to generate, store and distribute energy to the different parts of the telescope at all phases of its life. Table 7 resumes the two different power consumption expected during the mission. The first column refers to the nominal functioning of the satellite: the optical system is activated and the results are communicated with the Earth's ground stations. The AOCS adapt constantly the orientation of the spacecraft to counterbalance the loads. The propulsion system is also considered in the case an impulse is required to take on the effects of the reaction wheel during the desaturation process. The thermal system maintains the temperature of each part in its working temperature range.

The second case is the worst-case scenario and determines the solar arrays and battery sizing. It represents the journey of the spacecraft to L2 with the thermal system cooling down all the spacecraft, the propulsion system at its peak power and the AOCS working under maximal capacities. The battery sizing takes into account a 30 min deployment of the solar arrays and

provides the necessary power, with a 20% margin on the worst-case scenario. They are made of Li-Ion with a total weight of 10.75 kg. The solar arrays are made of triple-junction cells and size 6.65 m^2. A safe mode can also be considered with the optical system shut down and communication power reduced. The power is only used to preserve the spacecraft and it's orientation with the Sun.

	Power stand-by (W)	Power worst case (W)
AOCS power	33	315
Thermal power	95	400
Optic power	65	-
Data handling telecom	100	100
Propulsion	53	190
TOTAL	346	1005
w/ margin	433	1256

Table 7: Power budget evaluation

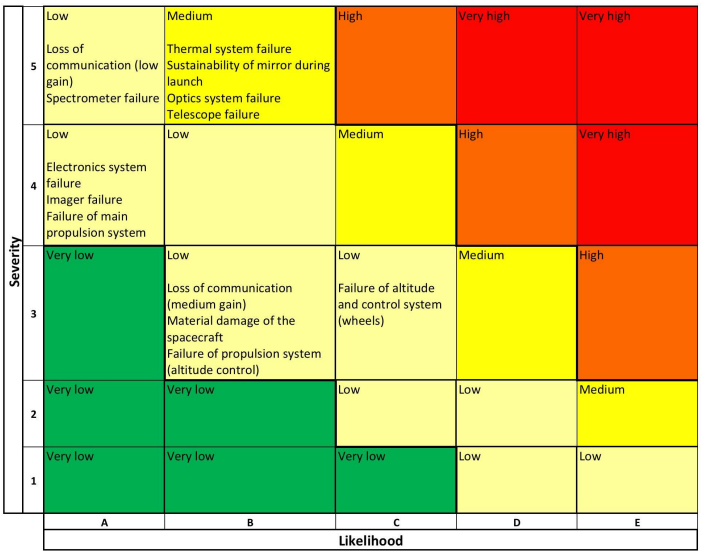

Figure 8: Comprehensive risk assessment for the ARISTOTLE mission.

14 Ground Testing & Design Models

Ground testing & qualification is essential to ensure the spacecraft's proper functioning under harsh environments. The tests can be categorised into three parts:

- Functional tests: Includes structural test, optical verification, electrical test, etc.
- Launch tests: Vibration test, acoustic noise test, and shock test.
- Orbital environment tests: Thermal vacuum test, radiation test, electromagnetic compatibility test.

Depending on the model/test philosophy, the tests on the instruments and the spacecraft could be performed combined or separately.

15 Ground and Launch Segment

The ground segment used for the ARISTOTLE mission consists of the Mission Operation Centre (MOC) conducting spacecraft operations, the Science Ground Segment (SGS) performing science data processing and the ESTRACK deep space ground station network used for telecommunication. The ARISTOTLE spacecraft is launched using the ARIANE 62 launcher, which has the capability to deliver payloads of up to 3300 kg to L2.

16 Risk Assessment

Despite conservative estimates, the highest risk rating for any of the components in the space mission is "Medium". This is due to the fact that the majority of the components in the spacecraft have well known heritage and there are also a number of mitigations in place for equipment which have proven to be less reliable in previous missions.

17 Cost Estimation

The cost estimation for ARISTOTLE is based on the analogy approach / benchmarking with the comparable ESA-Mission Herschel. For the cost analysis a cost correction factor of 0.28% was taken into account. Table 8 shows that ARISTOTLE's total ESA costs are below the limit of €1300M, classifying ARISTOTLE as an L-class mission according to ESA standards.

ARISTOTLE's cost element	%	**Costs [M€]**
ESA space segment	50	625
Mission / science operations	15	187.5
ESA project team overhead	12	150
Ariane 62 launcher	8	100
Margin	15	187.5
Sum ESA costs (L-mission limit 2023: 1,300 M€)	100	1,250
Payload costs of member states (roughly 30% of ESA costs)	30	361.5
Overall mission costs		**1,611.5**

Table 8: ARISTOTLE's cost breakdown

18 Conclusion

With a 4m dish, great thermal performance, and a spectrograph covering wavelengths of $2.5 - 23\mu m$, ARISTOTLE will vastly increase our understanding of exoplanet atmospheres. Building on transiting exoplanets discovered by the future PLATO mission, ARISTOTLE will especially focus on fainter and colder exoplanets, potentially all the way down to some super-Earths in the habitable zone. ARISTOTLE employs a larger dish and a wider frequency band than ARIEL, and hopes to learn from systematic errors and drawbacks in the MIRI instrument. Combining this with repeating transits and eclipses, the mission will access fainter planets with unprecedented accuracy.

In addition, ARISTOTLE will investigate protoplanetary disks, the lower atmospheres of Uranus and Neptune, Solar System moons and comets, which will all contribute to our understanding of exoplanetary systems, as well as our own Solar System.

References

[1] Esa space debris mitigation compliance verification guidelines. ESA. Accessed: 2023-07-19.

[2] James Webb's MIRI instrument cryocooler. https://webb.nasa.gov/content/about/innovations/cryocooler.html. Accessed: 2023-07-19.

[3] JPL, NASA: Why study comets? https://ssd.jpl.nasa.gov/sb/why_comets.html. Accessed: 2023-07-19.

[4] Nasa: Exoplanet exploration: Planets beyond our solar system. https://exoplanets.nasa.gov/discovery/how-we-find-and-characterize/#:~:text=It%27s%20a%20technique%20known%20as,tells%20about%20where%20it%27s%20been. Accessed: 2023-07-19.

[5] The PLATO mission. https://platomission.com/. Accessed: 2023-07-19.

[6] A. Antunes. Exploring deep-sea brines as potential terrestrial analogues of oceans in the icy moons of the outer solar system. *Current Issues in Molecular Biology*, 38:123–162, jan 2020.

[7] J. Barnes. Science goals and objectives for the dragonfly titan rotorcraft relocatable lander. *The Planetary Science Journal*, 2, jul 2021.

[8] W. J. Borucki. Kepler mission: development and overview. *Reports on Progress in Physics*, 79(3):036901, feb 2016.

[9] V. Bozza, L. Mancini, and A. Sozzetti. *Astrophysics of Exoplanetary Atmospheres: 2nd Advanced School on Exoplanetary Science*. Astrophysics and Space Science Library. Springer International Publishing, 2018.

[10] H. e. a. Daneshvar. Multilayer radiation shield for satellite electronic components protection. *Scientific Reports*, 11(1):20657, 2021.

[11] T. Das. Insights into the origin of life: Did it begin from hcn and h2o? *American Chemical Society Central Science*, 5:1532–1540, aug 2019.

[12] D. J. M. P. dit de la Roche et al. New constraints on the HR 8799 planetary system from mid-infrared direct imaging. *Monthly Notices of the Royal Astronomical Society*, 491(2):1795–1799, nov 2019.

[13] D. J. M. P. dit de la Roche et al. New mid-infrared imaging constraints on companions and protoplanetary disks around six young stars. *Astronomy &amp Astrophysics*, 648:A92, apr 2021.

[14] C. Dullemond and J. Monnier. The inner regions of protoplanetary disks. *Annual Review of Astronomy and Astrophysics*, 48(1):205–239, 2010.

[15] ESA. Ariel definition study report. https://sci.esa.int/web/ariel/-/ariel-definition-study-report-red-book. Accessed: 2023-07-19.

[16] A. E. S. N. et al. Review of state-of-the-art green monopropellants: For propulsion systems analysts and designers. *Aerospace*, 8(1), 2021.

[17] A. V. P. et al. Broadband quantum spectroscopy at the fingerprint mid-infrared region. *ACS Photonics*, 9(6):2151–2159, 2022.

[18] B. C. et al. A survey of exoplanet phase curves with ariel. *Experimental Astronomy*, 53(2):417–446, mar 2021.

[19] B. M. M. et al. The stellar variability noise floor for transiting exoplanet photometry with iPLATO/i. *Monthly Notices of the Royal Astronomical Society*, 493(4):5489–5498, mar 2020.

[20] D. G. et al. JWST MIRI/MRS in-flight absolute flux calibration and tailored fringe correction for unresolved sources. *Astronomy &amp Astrophysics*, 673:A102, may 2023.

[21] D. W. et al. Comet grains and implications for heating and radial mixing in the protoplanetary disk. *Conference paper*, 2007.

[22] E. W. S. et al. Exoplanet biosignatures: A review of remotely detectable signs of life. *Astrobiology*, 18(6):663–708, 2018.

[23] G. H. R. et al. The mid-infrared instrument for theijames webb space telescope/i, VII: The MIRI detectors. *Publications of the Astronomical Society of the Pacific*, 127(953):665–674, jul 2015.

[24] G. R. R. et al. Transiting Exoplanet Survey Satellite (TESS). *Journal of Astronomical Telescopes, Instruments, and Systems*, 1:014003, Jan. 2015.

[25] G. S. W. et al. The mid-infrared instrument for jwst and its in-flight performance. *Publications of the Astronomical Society of the Pacific*, 135(1046):048003, may 2023.

[26] G. T. et al. Ariel: Enabling planetary science across light-years, 2021.

[27] H. R. et al. The plato mission. *Astronomische Nachrichten*, 337(8-9):961–963, 2016.

[28] K. W. et al. Imaging low-mass planets within the habitable zone of centauri. *Nature Communications*, 12(1), feb 2021.

[29] M. K. et al. Near: Low-mass planets in α cen with visir. *The Messenger*, 169:16–20, Sept. 2017.

[30] M. K. et al. Predicting the exoplanet yield of the TESS prime and extended missions through years 1–7. *The Astronomical Journal*, 163(6):290, may 2022.

[31] M. M. et al. Origins space telescope mission concept study report, 2019.

[32] P. P. et al. High-contrast imaging at ten microns: A search for exoplanets around eps indi a, eps eri, tau ceti, sirius a, and sirius b. *Astronomy &amp Astrophysics*, 652:A121, aug 2021.

[33] S. A. et al. Understanding the evolution of radiation damage on the Gaia CCDs after 72 months at L2. *Journal of Astronomical Telescopes, Instruments, and Systems*, 8(1):016003, 2022.

[34] EUROSPACE. Revised space industry position 2020:exemption of propellant-related use of hydrazine and other liquid propellants from the reach authorisation requirement.

[35] L. Fletcher. Jupiter science enabled by esa's jupiter icy moons explorer. *arXiv [astro-ph.EP]*, 2023.

[36] T. Guillot. Uranus and neptune are key to understand planets with hydrogen atmospheres. *White Paper for ESA's Voyage 2050*, 2019.

[37] R. Helled. The interiors of uranus and neptune: current understanding and open questions. *Philosophical Transactions of the Royal Society A*, 378, nov 2020.

[38] R. Heller. Formation, habitability, and detection of extrasolar moons. *Astrobiology*, 14:798–835, sep 2014.

[39] A. J. McKay and N. X. Roth. Organic matter in cometary environments. *Life*, 2021.

[40] S. Quanz. Atmospheric characterization of terrestrial exoplanets in the mid-infrared: biosignatures, habitability, and diversity. *Experimental Astronomy*, 54:1197–1221, sep 2021.

[41] D. Sasselov. The origin of life as a planetary phenomenon. *Science Advances*, 6, feb 2020.

[42] S. Seager. Insights into the origin of life: Did it begin from hcn and h2o? *The Astrophysical Journal*, 777:19, nov 2013.

[43] S. Seager and D. D. Sasselov. Theoretical transmission spectra during extrasolar giant planet transits. *The Astrophysical Journal*, 537(2):916–921, jul 2000.

[44] A. Shields. Energy budgets for terrestrial extrasolar planets. *The Astrophysical Journal Letters*, 884, oct 2019.

[45] C. Sousa-Silva. Phosphine as a biosignature gas in exoplanet atmospheres. *Astrobiology*, 20, jan 2020.